Comparison of Magneto-Gravitational and Optical Trapping for Levitated Optomechanics

Charles W. Lewandowski, Wm. Randall Babbitt, and Brian D'Urso

Montana State University, P.O. Box 173840, Bozeman MT, USA

ABSTRACT

Levitated optomechanics in vacuum has shown promise for fundamental tests of physics including quantum mechanics and gravity, for sensing weak forces or accelerations, and for precision measurements. While much research has focused on optical trapping of dielectric particles, other approaches, such as magnetic trapping of diamagnetic particles, have been gaining interest. Here we review geometries for both optical and magnetic trapping in vacuum, with an emphasis on the properties of traps for particles with a diameter of at least one micrometer.

Keywords: magnetic trapping, optical trapping, levitated optomechanics

1. INTRODUCTION

Optical trapping has dominated research in levitated optomechanics with mesoscopic objects, but interest in extending the accessible parameter regimes has led to investigations into new trapping techniques, including magnetic, magneto-gravitational, and Paul (also known as RF or ion) trapping. Here, we compare the properties of optical and magnetic traps, with a particular emphasis on their properties when trapping particles have diameters of 1 μm or larger in vacuum.

There are two primary configurations of optical traps commonly used with larger particles. In the first, developed in the 1970s,[1] a single focused beam is oriented with the direction of propagation anti-parallel to the force of gravity, as shown in Fig. 1. Neodymium-doped YAG (Nd:YAG) lasers with wavelengths of 1064 nm are frequently used because of their large availability and high optical powers. The scattering force on the particle from the trapping beam helps counteract gravity, while the gradient force pulls the particle back to the center, resulting in a stable trap. The second optical trap geometry uses counter propagating beams to cancel the scattering force, as shown in Fig. 2. Typically high numerical aperture (NA) objectives are typically used with high optical power (several milliWatts to Watts) to overcome the force of gravity. The significant difficulty in dual-beam optical traps is the need to align the two beams' overlap well.[2,3]

Recently, several diamagnetism-based traps have also been demonstrated in vacuum. The first magneto-gravitational trap configuration is based on a linear quadrupole magnetic field.[4–6] The trap, illustrated in Fig. 3, begins with a linear quadrupole field with its axis aligned with the z (axial) direction to confine the particle in the y (vertical) and x (transverse) directions. To confine the particle in the axial direction, the vertical symmetry of the trap is broken by either making the top pole pieces shorter than the bottom or curving the pole pieces gently up in the y-z plane. This reshapes the low-field region of the trap to follow a curve with a minimum in height (y) at the axial center of the trap. The result is that the earth's gravity pulls the particle to the center of the trap in the axial direction, creating a trap with full three-dimensional confinement. As implemented experimentally, the trap consists of four Hiperco-50A pole pieces with a typical saturation magnetization of 2.4 T. Two samarium-cobalt (SmCo) permanent magnets are placed between the pole pieces. The pole pieces concentrate the magnetic flux to a smaller region to increase the gradient of the magnetic field. In the axial direction, the top pole pieces are approximately 380 μm long and the bottom pole pieces are approximately 2.54 mm long. The gaps between the pole pieces are typically 75 μm in the transverse direction and 200 μm in the vertical direction.

Further author information: (Send correspondence to B.D.)
B.D.: E-mail: durso@montana.edu, Telephone: 1 406 994 3456

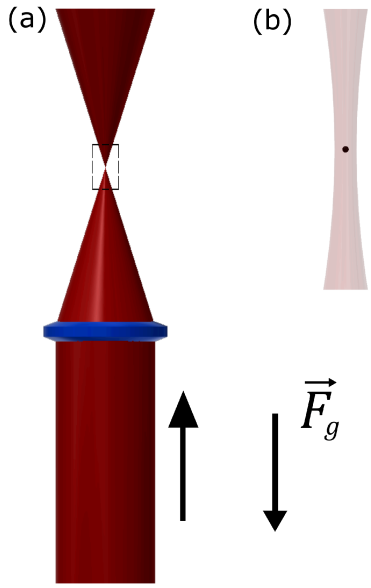

Figure 1. (a) An illustration of a single beam optical trap. The light propagation typically opposes gravity so the scattering force helps cancel gravity. The dielectric particle is pulled towards the electric field maximum, located at the focus of the beam. Typical trapping wavelengths are 1064 nm and 1550 nm. (b) A close up view of the trapping region as indicated by the black box in (a). The particle is not to scale to the demonstrated trapped particle sizes.

A linear quadrupole-based magneto-gravitational trap that has been extended in the axial direction has also been demonstrated as pictured in Fig. 4.[6] The four pole pieces are again made of Hiperco-50A and surround two SmCo magnets. In order to achieve lower oscillation frequencies in the axial direction, the dimension of the trap in that direction was increased to approximately 20 mm and 26 mm for the top and bottom pole pieces, respectively. The transverse and vertical gaps were increased to approximately 250 µm and 750 µm, respectively.

Another diamagnetic trap configuration, the axisymmetric scalable magneto-gravitation trap, is pictured in Fig. 5.[7] The trap consists of a neodymium-iron-boron (NdFeB) permanent magnet and two O1 tool steel pole pieces to concentrate the magnetic flux to a smaller region to increase the gradient of the magnetic field. The typical saturation magnetization is typically 1.0 T − 1.5 T. The bottom pole piece is conical with a tip radius of approximately 350 µm. The top pole piece is a hollow, cone shape with a bore-hole radius of approximately 350 µm. This hole allows particles to be loaded from the top of the trap. The top and bottom pole pieces are separated by a 350 µm gap. As with the linear quadrupole magneto-gravitational trap, gravity is required to form a trapping potential.

The last diamagnetic trap configuration we will examine is based on two permanent magnets and no pole pieces to levitate a particle without requiring gravity to form a stable trap.[8] This system is shown in Fig. 6. The cylindrical quadrupole magnetic trap has the advantage that it can be rotated since it does not depend on gravity to form the confining potential. The trap consists of two NdFeB permanent magnets with tips machined into four facets with an inclination of 28°, an angle which was determined to give the maximum vertical frequency and thus give the strongest trap. The two magnet tips are placed a distance of 30 µm apart with like poles of the magnets facing each other.

2. COMPARISONS

In this section, we compare several properties of trapped particles in these traps.

2.1 Trapped particle materials

Optical traps rely on a large gradient in an electric field produced by a tightly focused laser to levitate dielectric materials. Heating (potentially resulting in melting or vaporization) of trapped particles is a significant concern

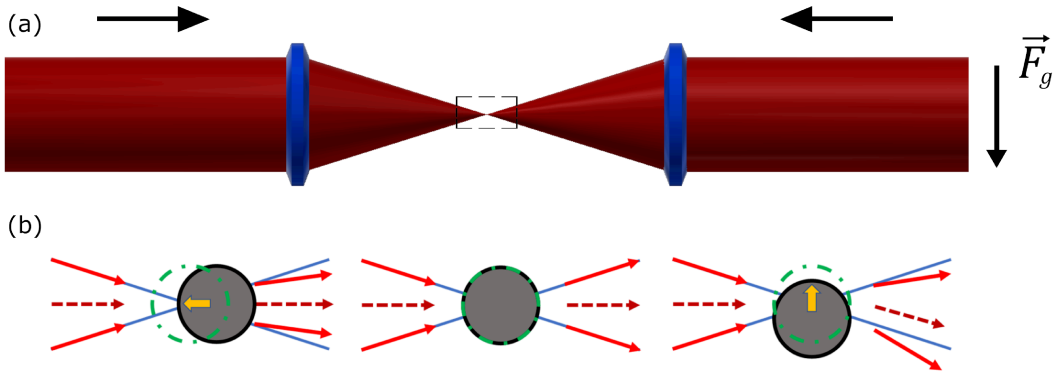

Figure 2. (a) An illustration of a dual beam optical trap. Unlike the single beam optical trap, careful alignment of both beams allows the scattering forces to cancel. This allows for higher trapping laser power (electric field gradient) and stronger restoring forces, deep well depths, and high oscillation frequencies. Large numerical apertures also contribute to these. Standard trapping wavelengths are 1064 nm and 1550 nm. (b) A view of the trapping region as indicated by the black box in (a) showing the rays of one of the trapping beams coming in from the left. Depending on the particle displacement from the center of the trap (indicated by dashed green circle), the rays change direction and transfer momentum to the particle, resulting in the gradient forces (yellow arrows). For a dual beam trap, these gradient forces add and the scattering forces (not shown) cancel. The strong gradient forces in the dual beam trap balance the gravitational force, with the equilibrium point slightly below the beam axis, as illustrated in right-most image.

in optical traps due to the high optical intensities utilized, so typically the trapped material must have very low absorption at the trapping wavelength. As the trapped particle travels through the gradient, there is a restoring force that pushes the particle back towards the highest intensity part of the beam. Common materials levitated in optical traps are silica (SiO_2)[9–27] and silicon (Si).[28] Diamonds[29,30] containing nitrogen vacancy (NV) centers are also of interest in trapping experiments because the manipulation of the defect centers can provide a quantum handle into the system,[31–33] though there is evidence they can graphitize and burn at sub-atmospheric pressures.[34] Optical trapping and rotation of a polymorph of calcium carbonate, vaterite (μ-$CaCO_3$), has also been demonstrated.[12] The birefringence nature of vaterite enhances the ability of light to rotate trapped spherical particles.

Magnetic traps have demonstrated trapping with a wider range of materials. For stable trapping, the particle must be diamagnetic ($\chi < 0$) so the particle is pushed towards the region with the weakest magnetic field. Any diamagnetic material can be levitated if the resulting trap is strong enough to overcome gravity, though insulators are preferred to prevent loss from eddy currents. The linear quadrupole magneto-gravitational trap has demonstrated the stable levitation of diamond, SiO_2, borosilicate glass, and silicon carbide (SiC).[4–6] In addition to the material reported in publications, we have observed that soda lime glass, dibutyl sebacate (DBS), silicone oils, water, isopropyl alcohol, polystyrene, vaterite, and graphite can been successfully trapped in linear quadrupole magneto-gravitational traps. The axisymmetric magneto-gravitational trap has demonstrated the levitation of gallium nitride (GaN) spheres and nanowires, SiO_2, and graphite powder.[7] The cylindrical quadrupole magnetic trap levitated diamonds, where it was observed that the frequency increased as a function of decreasing pressure, theorized as the magnetic susceptibility of diamond increasing as a function of temperature.[8]

2.2 Trapped particle sizes

Researchers have demonstrated levitation of particles with diameters of several hundred nanometers[11,17,22,24,28] and of several micrometers.[9,10,12–14,16,21] The most common diameters of particles in optical traps range from 100 nm to 150 nm.[18–20,25–27,29,30] Among the smallest particles that have been optically trapped in vacuum is a 26 nm diameter silica sphere.[23] Among the largest particles that have been optically trapped in vacuum are 20 µm diameter[15] and 30 µm diameter[35] silica microspheres.

With the linear quadrupole magneto-gravitational trap[4–6] trapping of silica microspheres approximately 1 µm to approximately 8 µm has been demonstrated. Nanodiamond clusters of approximately 3.5 µm have also been

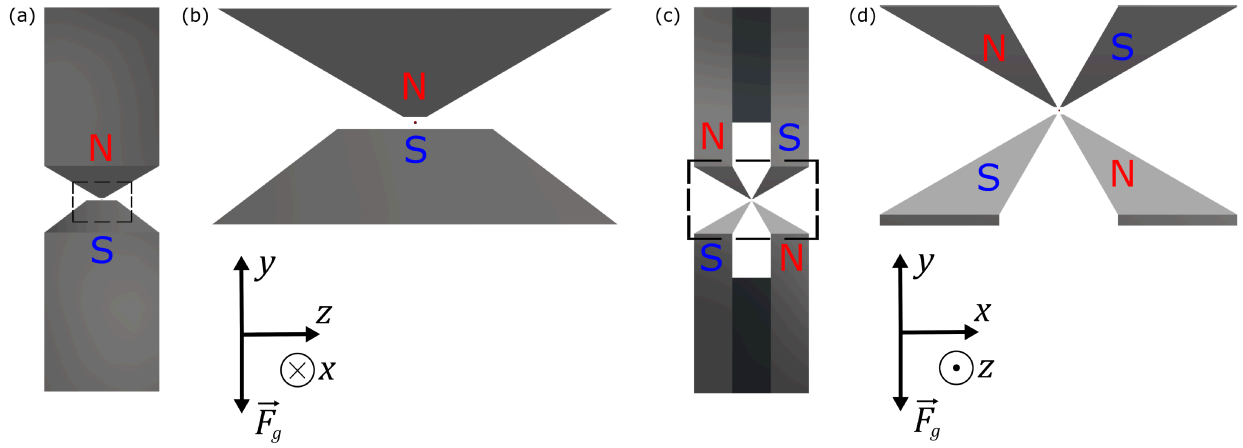

Figure 3. (a) The linear quadrupole magneto-gravitational trap[4–6] viewed from the transverse (x) direction. The trap consists of four Hiperco-50A pole pieces with a typical saturation magnetization of 2.4 T and SmCo permanent magnets. The vertical (y) gap is approximately 200 µm. The length along the top pole pieces in the axial (z) direction is approximately 380 µm and approximately 2.54 mm along the bottom pole pieces. (b) A close up view of the trapping region as indicated by the black box in (a). The particle is not to scale to the demonstrated trapped particle sizes. (c) The magneto-gravitational trap viewed from the axial direction. The transverse gap is approximately 75 µm. (d) A close up view of the trapping region as indicated by the black box in (c). The particle is magnetically bound in the transverse and vertical directions and magneto-gravitationally in the axial direction.

trapped. With the extended linear quadrupole magneto-gravitational trap[6] consistent trapping of borosilicate and soda lime glass microspheres from approximately 25 µm to approximately 65 µm has been achieved, as seen in Fig. 7. In the axisymmetric magneto-gravitational trap,[7] trapping has been demonstrated with many particle sizes. A 100 nm GaN particle can be trapped before thermal fluctuations are on the order of the trap depth. Silica microspheres of 6 µm diameter, GaN particles of 10 µm diameter, graphite powder with sizes between 50 µm and 300 µm, and GaN nanowires approximately 20 µm in length have also been trapped in this system. With the cylindrical quadrupole magnetic trap system,[8] trapping has been demonstrated with microdiamonds of approximately 1.5 µm to approximately 2.5 µm in diameter.

2.3 Center-of-mass oscillation frequencies

For a levitated particle of mass m in a harmonic potential, the oscillation frequency f of the particle is given by

$$f = \frac{\omega}{2\pi} = \frac{1}{2\pi}\sqrt{\frac{k}{m}}, \tag{1}$$

where ω is the angular frequency of the oscillation and k is the spring constant of the trap, which depends on the system being investigated.

In optical traps, the oscillation frequency mostly depends on particle size, the NA of focusing optics, and the trap geometry, as well as if motion is longitudinal or transverse to the trapping beam(s). Optical trapping systems typically have much higher center-of-mass oscillation frequencies than the magnetic trap and magneto-gravitational trap systems. Dual-beam and cavity optical traps typically can achieve much higher oscillation frequencies compared to single beam vertical optical traps. Typical values in an optical trap with sub-micron diameter particles are $f \approx 100 - 200kHz$.[12,18,20,21,24–29] The highest reported center-of-mass frequency to our knowledge is $f \approx 300$ kHz for a 26 nm silica nanosphere in vacuum.[23] Center-of-mass frequencies in an optical trap have been reported as low as $f \approx 20$ Hz for a 20 µm silica microsphere in vacuum.[15,16]

The magnetic trap and magneto-gravitational trap systems have significantly lower oscillation frequencies than optical traps because the magnetic susceptibilities of diamagnetic materials are generally much smaller in magnitude than the electric susceptibilities of dielectric materials. The lowest frequency demonstrated in a

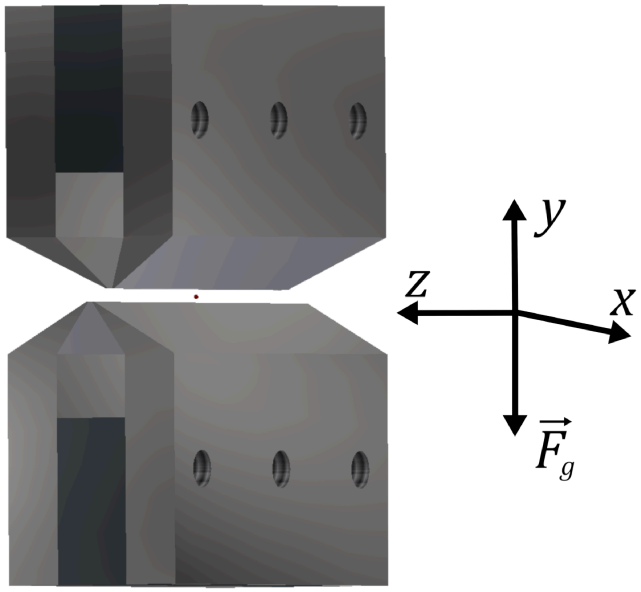

Figure 4. The extended linear quadrupole magneto-gravitational trap.[6] Similar to the trap in Fig. 3,[4–6] this system consists of four Hiperco-50A pole pieces and SmCo permanent magnets. The vertical (y) gap is approximately 750 µm and the gap in the transverse (x) direction is approximately 250 µm. Lower frequencies in the axial (z) direction are achieved due to the extended length of the pole pieces in that direction. The top pole piece is approximately 20 mm and the bottom pole piece is approximately 26 mm in the axial direction. The particle is not to scale to the demonstrated trapped particle sizes.

magnetic based trap is $f \approx 0.25$ Hz in the extended linear quadrupole trap as shown in Fig. 4.[6] The low frequency is due to the large dimension in the axial (z) direction. In this trap system, the frequency in the vertical (y) direction is $f \approx 10$ Hz. An accurate measurement of the transverse (x) direction oscillation frequency has not obtained. In the shorter linear quadrupole trap pictured in Fig. 3,[4–6] the center-of-mass oscillation frequencies in the axial, vertical, and transverse directions are $f_z \approx 7$ Hz, $f_y \approx 100$ Hz, and $f_x \approx 60$ Hz, respectively. The axial center-of-mass frequency can be arbitrarily low in this system without loss of trap depth by extending the axial dimension of the trap.

The axisymmetric scalable magneto-gravitational trap[7] as shown in Fig. 5 has reported similar frequencies to the linear quadrupole trap. In the vertical direction, a frequency of $f_v \approx 30$ Hz is demonstrated. Because of the cylindrical symmetry, the particle oscillates in all directions radially at a frequency of $f_r \approx 25$ Hz. The cylindrical quadrupole magnetic trap system[8] shown in Fig. 6 has higher frequencies reported. In the horizontal directions, the frequencies are $f_h \approx 200$ Hz. In the vertical direction, the frequency is twice as large at $f_v \approx 400$ Hz.

2.4 Maximum center-of-mass oscillation amplitudes

For optical trapping systems with the particle radius, r_p, much less than the trapping wavelength, $r_p \ll \lambda$ (the Rayleigh scattering regime), the maximum center-of-mass oscillation amplitude r_{max} (over which range the trap force changes roughly linearly) is roughly the beam waist w_0 of the trapping laser, $r_{max} \approx w_0$. Because gravity opposes the scattering force on the particles in a single-beam vertical optical trap, lower NAs can be used, increasing the beam waist and thus the maximum oscillation amplitude. For example, a single-beam trap using a 1064 nm laser with $r_{max} \approx w_0 \approx 25$ µm has been reported.[35] For dual-beam horizontal optical traps, NAs of approximately 0.8 are typical. For a 1064 nm laser, the high NA results in $r_{max} \approx w_0 \approx 420$ nm.

For optical trapping systems with $r_p \gg \lambda$, larger center-of-mass oscillation amplitudes can be achieved. Using the Optical Tweezers in Geometrical Optics (OTGO) software developed by Callegari et al [36] that was modified by St. John[3] to handle a variety of trap geometries and compute potential wells and further adapted here to analyze oscillation frequencies and well depths, an empirical formula for the maximum center-of-mass oscillation

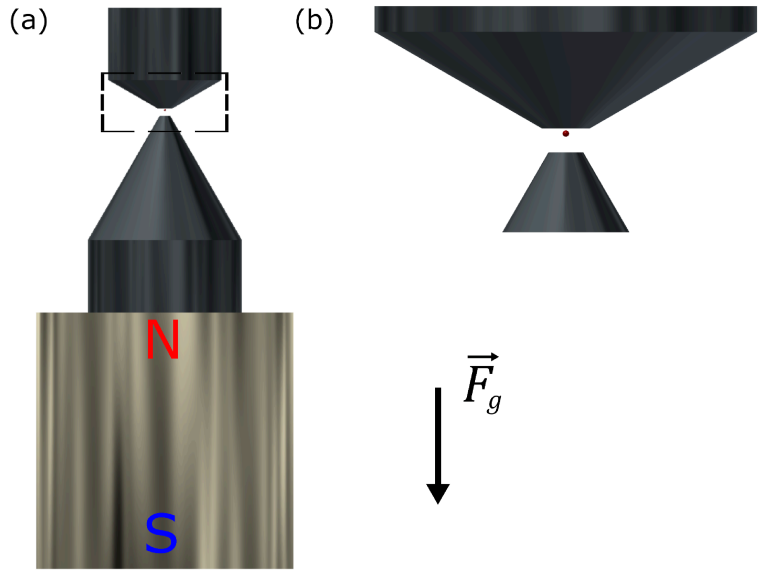

Figure 5. (a) The axisymmetric scalable magneto-gravitational trap.[7] The bottom pole piece concentrates the magnetic flux from the NdFeB permanent magnet. The top pole piece contains a bore-hole down the center to allow particles to be dropped in from the top for loading. The two pole pieces are made of O1 tool steel with a typical saturation magnetization of $1.0\,\mathrm{T} - 1.5\,\mathrm{T}$. The vertical gap and the radius of the flat tip of the bottom pole piece are approximately $350\,\mu\mathrm{m}$. The bottom pole piece has a 60° taper and the top pole piece has a taper of 30°. (b) A close up view of the trapping region as indicated by the black box in (a). The particle is not to scale to the demonstrated trapped particle sizes.

amplitude r_{max} in the longitudinal and transverse directions were found. The maximum transverse oscillation amplitude for $r_p \gg \lambda$ is approximately twice the particle radius, $r_{max} \approx 2r_p$, for both vertical and horizontal traps. The maximum longitudinal oscillation amplitude for $r_p \gg \lambda$ is given by $r_{max} = 2r_p/\mathrm{NA}$ for both vertical and horizontal traps. Thus, for a $10\,\mu\mathrm{m}$ diameter silica particles with $\mathrm{NA} = 0.5$, $r_{max} \approx 10\,\mu\mathrm{m}$ for transverse motion and $r_{max} \approx 20\,\mu\mathrm{m}$ for longitudinal motion.

The linear quadrupole magneto-gravitational trap[4–6] consists of four pole pieces that limit the amplitude of motion for the levitated particle. In the transverse (x) direction, the particle's amplitude is approximately limited by the distance from the distance between the centers of the tips of the pole pieces, $x_{max} \approx 125\,\mu\mathrm{m}$. The vertical ($y$) direction amplitude is limited by the vertical gap of the trap, $y_{max} \approx 100\,\mu\mathrm{m}$. A good estimate for the maximum amplitude in the axial (z) direction is half of the length of the top pole pieces, $z_{max} \approx 190\,\mu\mathrm{m}$. Based on similar arguments, the extended linear quadrupole trap has amplitudes in the transverse, vertical, and axial directions are $x_{max} \approx 250\,\mu\mathrm{m}$, $y_{max} \approx 375\,\mu\mathrm{m}$, and $z_{max} \approx 10.5\,\mathrm{mm}$, and an oscillation amplitude of approximately $10\,\mathrm{mm}$ has been demonstrated. In principle, arbitrarily large amplitudes in the axial direction can be achieved by extending the axial dimension of the trap.

The axisymmetric scalable magneto-gravitational trap[7] has a potential minimum located in the center of the trap radially and near the tip of the top, nozzle shaped pole piece where a neutral particle will be positioned. In the radial direction, the particle is limited by the physical boundary of the pole piece, $r_{max} \approx 350\,\mu\mathrm{m}$. In the vertical direction, the particle is constrained to $y_{max} \approx 200\,\mu\mathrm{m}$. The two magnets in the cylindrical quadrupole magnetic trap system were separated vertically by a distance of $30\,\mu\mathrm{m}$. In this direction, the particle's amplitude is limited by the magnets, $y_{max} \approx 15\,\mu\mathrm{m}$. In the horizontal directions, a conservative estimate for the maximum amplitude to be on the order of the size of the vertical gap, $x_{max} \sim y_{max} \sim 30\,\mu\mathrm{m}$.

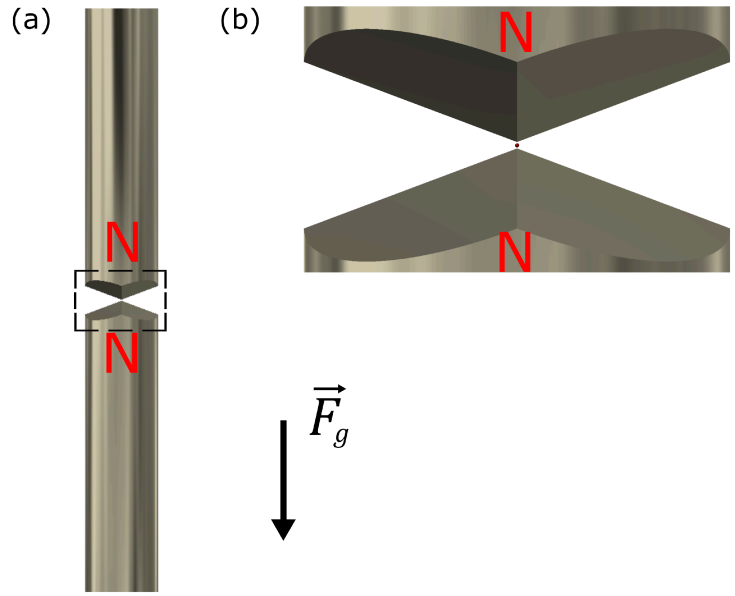

Figure 6. (a) The cylindrical quadrupole magnetic trap system.[8] The trap consists of two NdFeB permenant magnets with the same poles together. The magnet tips are machined into four facets with an inclination of 28° to give the maximum vertical frequency. The tips are separated by a distance of 30 µm. (b) A close up view of the trapping region as indicated by the black box in (a). The particle is not to scale to the demonstrated trapped particle sizes. Unlike the traps in Fig. 5,[7] Fig. 3,[4–6] and Fig. 4,[6] the particle is not bound by gravity allowing this trap to be rotated.

2.5 Trap depth (escape energy)

The trap depth temperature T_{max} in an optical trapping system where the radius of a levitated sphere is much smaller than the trapping wavelength, $r_p \ll \lambda$, is given by[37]

$$k_B T_{max} = \frac{3 I_0 V}{c} \mathrm{Re}\left\{\frac{\epsilon - 1}{\epsilon + 2}\right\}, \tag{2}$$

where I_0 is the intensity of the trapping laser, V is the sphere volume, c is the speed of light in vacuum, and ϵ is the electric permittivity of the particle. For typical optical parameters of optical power ≈ 0.5 W, beam waist ≈ 500 nm, and a SiO_2 particle with 150 nm diameter and electric permittivity $\epsilon = 3.9$, a trap depth can be estimated at $T_{max} \sim 10^7$ K. Therefore, even for relatively small particles, the trap depth in optical traps is usually much larger than room temperature. For optical trapping systems with $r_p \gg \lambda$, we again employed the modified OTGO software developed by Callegari et al [36] and St. John[3] to estimate trap depth temperatures. For a 10 µm diameter silica particle in both vertical and dual-beam horizontal traps with a 1064 nm trapping wavelength, NA = 0.5, and beam powers of $25 - 100$ mW, we found $T_{max} \sim 10^7 - 10^8$ K, with oscillation frequencies of $0.1 - 1$ kHz.

For the linear quadrupole magneto-gravitational trap,[5] the trap depth is limited to the energy of the particle displaced to the edge of the trap axially. For the trap in Fig. 3, $z_{lim} \approx 190$ µm. For a particle of mass m oscillating with angular frequency ω_z in the axial direction,

$$k_B T_{max} = \frac{1}{2} m \omega_z^2 z_{lim}^2. \tag{3}$$

For a 1.5 µm SiO_2 sphere oscillating with frequency $\omega_z/2\pi \approx 7$ Hz, $T_{max} \approx 8000$ K. The axial oscillation frequency can be made arbitrarily small while keeping the trap depth large enough by increasing the length of the trap in the axial direction. In the extended linear quadrupole magneto-gravitational trap,[6] typical particles are 65 µm diameter SiO_2 spheres that oscillate at a frequency of $\omega_z/2\pi \approx 0.25$ Hz. By Eq. 3, the trap depth is

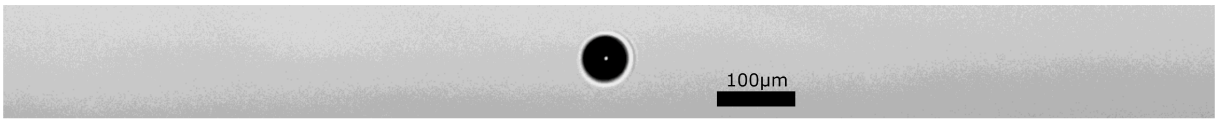

Figure 7. A 60 μm particle levitated in the extended linear quadrupole magneto-gravitational trap illustrated in Fig. 4. The particle is stroboscopically illuminated by a 660 nm LED and imaged onto a CMOS camera.

$\sim 10^{11}$ K. In the axisymmetric magneto-gravitational trap, it is reported that for a 10 μm GaN sphere, the trap depth is estimated to be $\sim 10^6$ K.[7] GaN particles down to approximately 100 nm can be trapped before thermal fluctuations are comparable to the trap depth. A similar analysis can be performed for the cylindrical quadrupole magnetic trap system[8] to that of the linear quadrupole magneto-gravitational trap. In the horizontal directions, a conservative limit on the maximum amplitude is on the order of the vertical gap, $x_{lim} \sim y_{lim} \sim 30$ μm. Assuming a sphere, a diamond of diameter 2.0 μm oscillating horizontally with a frequency of $\omega_h/2\pi \approx 200$ Hz will have a trap depth of 600, 000 K, determined by Eq. 3.

2.6 Chamber pressure

Optical trapping systems have been studied since the 1970s, with the majority of the work focused on trapping in liquid and air. For sensitive measurements and to reach the quantum limit of the COM motion, collisions with air molecules must be minimized, requiring trapping in vacuum. Optical trapping in vacuum typically requires active cooling of the COM motion to avoid particle loss due to radiometric forces exacerbated by differential particle heating .[2,15] Trapping has been successful with SiO_2 and Si from atmospheric pressure down to $\sim 10^{-8}$ Torr.[26,28] Nanodiamonds have been levitated down to a pressure on the order of a few Torr,[29] and vaterite spheres have been trapped down to a pressure of $\sim 10^{-7}$ Torr.[12]

Because of the passive nature of the magnetic based traps, in principle it is possible to have a levitated particle remain trapped indefinitely at any pressure. The linear quadrupole magneto-gravitational trap has reported what may be the lowest pressures of any levitated optomechanical trapping experiment, demonstrating levitation of a SiO_2 microsphere at ultra-high vacuum, with a pressure of $\sim 10^{-10}$ Torr.[5] The axisymmetric magneto-gravitational trap reported levitation at a pressure of ~ 0.001 Torr.[7] The cylindrical quadrupole magnetic trap has demonstrated trapping of microdiamonds down to a pressure of ~ 0.1 Torr.[8] Though NdFeB permanent magnets are stronger than SmCo permanent magnets, the Curie temperature of NdFeB permanent magnets limits how hot the systems can be baked to achieve lower pressures. As a result, the cylindrical quadrupole magnetic trap and the axisymmetric magneto-gravitational traps would likely need some modification to reach ultra-high vacuum.

2.7 Cooling the center-of-mass motion

In 1977, Ashkin and Dziedzic reported cooling the motion of 10.8 μm, 8.7 μm, and 4.1 μm diameter particles levitated in a single-beam vertical optical in high vacuum by modulating the power of the trapping laser proportional to the vertical velocity of the particle as detected on a split photodiode.[16] This process, typically known as "cold damping" or linear feedback cooling, primarily uses the modulated scattering force of the laser to provide the damping force. The horizontal motions of the particle were incidentally damped in the same process. Full three-dimensional cooling of a 3 μm silica microsphere in vacuum to a minimum temperature of 1.5 mK has further been demonstrated.[38]

The scattering force is typically not used for feedback with smaller, optically trapped particles (which are beyond the primary scope of this paper). Instead, the optical gradient force can be used for parametric (non-linear) feedback (e.g.[20]), or charged particles can been cooled with the Coulomb force,[26,39] reaching motional temperatures down to 100 μK in one degree of freedom.[26]

Feedback cooling has also been demonstrated in traps based on diamagnetism, including cold damping with a feedback force from the magnetic field generated by a modulated current in a wire[4] or the optical scattering force from a control beam,[5] with the latter reaching motional temperatures down to 600 μK in one degree of freedom of a trapped 1.54 μm diameter silica particle.

2.8 Size of quantum ground state

The zero-point motion sets the size of the ground state in a quantum harmonic oscillator (QHO). For a QHO in the z-direction for a with mass m and angular frequency ω_z, the size of the ground state is

$$z_0 = \sqrt{\langle z^2 \rangle} = \sqrt{\frac{\hbar}{2m\omega_z}}. \tag{4}$$

For a typical SiO_2 sphere in a linear quadrupole magneto-gravitational trap with a diameter of 1.5 µm and frequency $\omega_z/2\pi = 7\,\text{Hz}$, $z_0 \approx 2 \times 10^{-11}$ m. In optical traps, the typical size of particles is much smaller at approximately 150 nm with frequencies typically on the order of $\omega/2\pi \approx 150\,\text{kHz}$. For a spherical SiO_2 particle, by Eq. 4, $z_0 \approx 1.2 \times 10^{-12}$ m. For the cylindrical quadrupole magnetic trap system[8] with a levitated 2 µm diamond at frequencies of approximately 200 Hz, the zero-point extension is approximately 1.5×10^{-12} m.

2.9 Force and acceleration sensitivity

The force sensitivity of a spherical harmonic oscillator of mass m is given by[11]

$$S_F^{1/2} = \sqrt{4k_B T m \Gamma} \tag{5}$$

where Γ is the damping rate of the oscillator at temperature T. Since the use of feedback to add cold damping can at best maintain the product ΓT constant, it cannot improve the force sensitivity. Dividing Eq. 5 by m gives the acceleration sensitivity.

$$S_a^{1/2} = \sqrt{\frac{4k_B T \Gamma}{m}} \tag{6}$$

Generally, the use of larger particles allow for better acceleration sensitivity, whereas smaller particles allow for better force sensitivity.

With optical trapping, force sensitivity of approximately 6×10^{-21} N over a time of 10^5 s has been reported.[11] This gives $S_F^{1/2} \sim 10^{-18}$ $\text{NHz}^{-1/2}$. With the 300 nm diameter SiO_2 particle used, an acceleration sensitivity of approximately $S_a^{1/2} \approx 5 \times 10^{-2}$ $\text{ms}^{-2}\text{Hz}^{-1/2}$ can be estimated. An acceleration sensitivity of $S_a^{1/2} \approx 7.5 \times 10^{-5}$ $\text{ms}^{-2}\text{Hz}^{-1/2}$ has also been reported[9] with a larger particle in a vertical beam trap. By multiplying by the mass of the 4.8 µm diameter SiO_2 sphere, the force sensitivity is $S_F^{1/2} \sim 10^{-17}$ $\text{NHz}^{-1/2}$.

For a 1.5 µm diameter SiO_2 particle in the linear quadrupole magneto-gravitational trap, the damping is estimated to be $\Gamma \approx 10^{-5}$ s^{-1}.[5] From Eq. 5, we get $S_F^{1/2} \sim 10^{-20}$ $\text{NHz}^{-1/2}$. The acceleration sensitivity for this particle is $S_a^{1/2} \sim 10^{-6}$ $\text{ms}^{-2}\text{Hz}^{-1/2}$.

3. CONCLUSIONS

A comparison of the properties of particles in optical and diamagnetic traps reveals that each has advantages, with largely complementary features. Optical traps are typically stiffer and deeper, enabling much higher oscillation frequencies and much smaller particles than diamagnetic traps. However, the high NA of objective lenses often used to focus the trapping beam results in a relatively small trapping region and thus a small maximum oscillation amplitude. Diamagnetic traps are typically much less stiff, resulting in lower oscillation frequencies. They can still reach manageable trap depths by being much larger, with almost arbitrarily large oscillation amplitudes possible and at least 1 cm amplitude demonstrated. Diamagnetic traps have also been demonstrated with somewhat larger particles than optical trapping, and also feature passive stability at all background pressures and less strict requirements on the transparency of particles. In practice, the choice of trap type and geometry will depend on the desired characteristics of the system.

ACKNOWLEDGMENTS

This material is based upon work supported by the National Science Foundation under Grant No. 1757005, 1827071, and 1912083, and a block gift from the II-VI Foundation. The authors are grateful for the work by Brianne Malchow for compiling data from optical levitation references.

REFERENCES

[1] Ashkin, A., "Acceleration and trapping of particles by radiation pressure," *Phys. Rev. Lett.* **24**(4), 156 (1970).

[2] Atherton, D. P., *Sensitive Force Measurements with Optically Trapped Micro-Spheres in High Vacuum*, PhD thesis, University of Nevada, Reno (2015).

[3] St John, D. R. et al., *Theoretical analysis and experimental design of dual-beam optical trap for large particles*, PhD thesis, Montana State University-Bozeman, College of Letters & Science (2018).

[4] Hsu, J.-F., Ji, P., Lewandowski, C. W., and D'Urso, B., "Cooling the motion of diamond nanocrystals in a magneto-gravitational trap in high vacuum," *Sci. Rep.* **6**, 30125 (2016).

[5] Slezak, B. R., Lewandowski, C. W., Hsu, J.-F., and D'Urso, B., "Cooling the motion of a silica microsphere in a magneto-gravitational trap in ultra-high vacuum," *New J. Phys.* **20**, 063028 (2018).

[6] Klahold, W. M., Lewandowski, C. W., Nachman, P., Slezak, B. R., and D'Urso, B., "Precision optomechanics with a particle in a magneto-gravitational trap," in [*Optical, Opto-Atomic, and Entanglement-Enhanced Precision Metrology*], **10934**, 109340P, International Society for Optics and Photonics (2019).

[7] Houlton, J., Chen, M., Brubaker, M., Bertness, K., and Rogers, C., "Axisymmetric scalable magneto-gravitational trap for diamagnetic particle levitation," *Rev. Sci. Instrum.* **89**(12), 125107 (2018).

[8] O'Brien, M., Dunn, S., Downes, J., and Twamley, J., "Magneto-mechanical trapping of micro-diamonds at low pressures," *Appl. Phys. Lett.* **114**(5), 053103 (2019).

[9] Rider, A. D., Blakemore, C. P., Gratta, G., and Moore, D. C., "Single-beam dielectric-microsphere trapping with optical heterodyne detection," *Phys. Rev. A* **97**(1), 013842 (2018).

[10] Ranjit, G., Atherton, D. P., Stutz, J. H., Cunningham, M., and Geraci, A. A., "Attonewton force detection using microspheres in a dual-beam optical trap in high vacuum," *Phys. Rev. A* **91**(5), 051805 (2015).

[11] Ranjit, G., Cunningham, M., Casey, K., and Geraci, A. A., "Zeptonewton force sensing with nanospheres in an optical lattice," *Phys. Rev. A* **93**(5), 053801 (2016).

[12] Monteiro, F., Ghosh, S., van Assendelft, E. C., and Moore, D. C., "Optical rotation of levitated spheres in high vacuum," *Phys. Rev. A* **97**(5), 051802 (2018).

[13] Moore, D. C., Rider, A. D., and Gratta, G., "Search for millicharged particles using optically levitated microspheres," *Phys. Rev. Lett.* **113**(25), 251801 (2014).

[14] Li, T., "Millikelvin cooling of an optically trapped microsphere in vacuum," in [*Fundamental Tests of Physics with Optically Trapped Microspheres*], 81–110, Springer (2013).

[15] Ashkin, A. and Dziedzic, J., "Optical levitation in high vacuum," *Appl. Phys. Lett.* **28**(6), 333–335 (1976).

[16] Ashkin, A. and Dziedzic, J., "Feedback stabilization of optically levitated particles," *Appl. Phys. Lett.* **30**(4), 202–204 (1977).

[17] Millen, J., Fonseca, P., Mavrogordatos, T., Monteiro, T., and Barker, P., "Cavity cooling a single charged levitated nanosphere," *Phys. Rev. Lett.* **114**(12), 123602 (2015).

[18] Jain, V., Gieseler, J., Moritz, C., Dellago, C., Quidant, R., and Novotny, L., "Direct measurement of photon recoil from a levitated nanoparticle," *Phys. Rev. Lett.* **116**(24), 243601 (2016).

[19] Hempston, D., Vovrosh, J., Toroš, M., Winstone, G., Rashid, M., and Ulbricht, H., "Force sensing with an optically levitated charged nanoparticle," *Appl. Phys. Lett.* **111**(13), 133111 (2017).

[20] Gieseler, J., Deutsch, B., Quidant, R., and Novotny, L., "Subkelvin parametric feedback cooling of a laser-trapped nanoparticle," *Phys. Rev. Lett.* **109**(10), 103603 (2012).

[21] Mazilu, M., Arita, Y., Vettenburg, T., Auñón, J. M., Wright, E. M., and Dholakia, K., "Orbital-angular-momentum transfer to optically levitated microparticles in vacuum," *Phys. Rev. A* **94**(5), 053821 (2016).

[22] Fonseca, P., Aranas, E., Millen, J., Monteiro, T., and Barker, P., "Nonlinear dynamics and strong cavity cooling of levitated nanoparticles," *Phys. Rev. Lett.* **117**(17), 173602 (2016).

[23] Vovrosh, J., Rashid, M., Hempston, D., Bateman, J., Paternostro, M., and Ulbricht, H., "Parametric feedback cooling of levitated optomechanics in a parabolic mirror trap," *J. Opt. Soc. Am. B* **34**(7), 1421–1428 (2017).

[24] Kiesel, N., Blaser, F., Delić, U., Grass, D., Kaltenbaek, R., and Aspelmeyer, M., "Cavity cooling of an optically levitated submicron particle," *Proc. Natl. Acad. Sci. U.S.A.* **110**(35), 14180–14185 (2013).

[25] Gieseler, J., Novotny, L., and Quidant, R., "Thermal nonlinearities in a nanomechanical oscillator," *Nat. Phys.* **9**(12), 806 (2013).

[26] Tebbenjohanns, F., Frimmer, M., Militaru, A., Jain, V., and Novotny, L., "Cold damping of an optically levitated nanoparticle to microkelvin temperatures," *Phys. Rev. Lett.* **122**(22), 223601 (2019).

[27] Windey, D., Gonzalez-Ballestero, C., Maurer, P., Novotny, L., Romero-Isart, O., and Reimann, R., "Cavity-based 3d cooling of a levitated nanoparticle via coherent scattering," *Phys. Rev. Lett.* **122**(12), 123601 (2019).

[28] Asenbaum, P., Kuhn, S., Nimmrichter, S., Sezer, U., and Arndt, M., "Cavity cooling of free silicon nanoparticles in high vacuum," *Nat. Commun.* **4**, 2743 (2013).

[29] Hoang, T. M., Ma, Y., Ahn, J., Bang, J., Robicheaux, F., Yin, Z.-Q., and Li, T., "Torsional optomechanics of a levitated nonspherical nanoparticle," *Phys. Rev. Lett.* **117**(12), 123604 (2016).

[30] Neukirch, L. P., Gieseler, J., Quidant, R., Novotny, L., and Vamivakas, A. N., "Observation of nitrogen vacancy photoluminescence from an optically levitated nanodiamond," *Opt. Lett.* **38**(16), 2976–2979 (2013).

[31] Doherty, M. W., Manson, N. B., Delaney, P., Jelezko, F., Wrachtrup, J., and Hollenberg, L. C., "The nitrogen-vacancy colour centre in diamond," *Phys. Rep.* **528**(1), 1–45 (2013).

[32] Horowitz, V. R., Alemán, B. J., Christle, D. J., Cleland, A. N., and Awschalom, D. D., "Electron spin resonance of nitrogen-vacancy centers in optically trapped nanodiamonds," *Proc. Natl. Acad. Sci. U.S.A.* **109**(34), 13493–13497 (2012).

[33] Yin, Z.-q., Li, T., Zhang, X., and Duan, L., "Large quantum superpositions of a levitated nanodiamond through spin-optomechanical coupling," *Phys. Rev. A* **88**(3), 033614 (2013).

[34] Rahman, A., Frangeskou, A., Kim, M., Bose, S., Morley, G., and Barker, P., "Burning and graphitization of optically levitated nanodiamonds in vacuum," *Sci. Rep.* **6**, 21633 (2016).

[35] Monteiro, F., Ghosh, S., Fine, A. G., and Moore, D. C., "Optical levitation of 10-ng spheres with nano-g acceleration sensitivity," *Phys. Rev. A* **96**(6), 063841 (2017).

[36] Callegari, A., Mijalkov, M., Gököz, A. B., and Volpe, G., "Computational toolbox for optical tweezers in geometrical optics," *J. Opt. Soc. Am. B* **32**(5), B11–B19 (2015).

[37] Chang, D. E., Regal, C., Papp, S., Wilson, D., Ye, J., Painter, O., Kimble, H. J., and Zoller, P., "Cavity opto-mechanics using an optically levitated nanosphere," *Proc. Natl. Acad. Sci. U.S.A.* **107**(3), 1005–1010 (2010).

[38] Li, T., Kheifets, S., and Raizen, M. G., "Millikelvin cooling of an optically trapped microsphere in vacuum," *Nat. Phys.* **7**(7), 527 (2011).

[39] Conangla, G. P., Ricci, F., Cuairan, M. T., Schell, A. W., Meyer, N., and Quidant, R., "Optimal feedback cooling of a charged levitated nanoparticle with adaptive control," *Phys. Rev. Lett.* **122**(22), 223602 (2019).